106589-81-5; KPb, 106589-82-6; $Pb_2Te_3^{2-}$, 106589-74-6; $Pb_2SeTe_2^{2-}$, 106589-75-7; $Pb_2Se_2Te^{2-}$, 106589-76-8; (2,2,2-crypt-K^+)$_2Pb_2Se_3^{2-}$, 106589-78-0; $Pb_2Se_3^{2-}$, 106589-77-9; K, 7440-09-7; Pb, 7439-92-1; Te, 13494-80-9; Se, 7782-49-2; ^{207}Pb, 14119-29-0; ^{77}Se, 14681-72-2; ^{125}Te, 14390-73-9.

Supplementary Material Available: Tables of anisotropic thermal parameters and of bond distances and bond angles in the 2,2,2-crypt moieties and Figure 3 (stereopair), showing the packing of (2,2,2-crypt-K^+)$_2Pb_2Se_3^{2-}$ (4 pages); a listing of final structure factor amplitudes (20 pages). Ordering information is given on any current masthead page.

Contribution from the Department of Chemistry and Biochemistry, University of Windsor, Windsor, Ontario, Canada N9B 3P4

Toward Copper(II) Hemocyanin Models. 2.† Synthesis and Characterization of Binuclear Copper(II) Complexes of a Heptadentate Ligand

Hilde P. Berends and Douglas W. Stephan*

Received August 28, 1986

The preparation of the heptadentate ligand 2,6-bis[(bis(benzimidazolylmethyl)amino)methyl]-*p*-cresol (**4**) is described. The preparation of the copper complex formulated as $[Cu_2L(H_2O)_2][ClO_4]_3 \cdot 3H_2O$ (**5**) (L = anion of **4**) is given. The products of substitution reactions involving replacement of the coordinated water molecules of **5** with *N*-methylimidazole, pyridine, formate, acetate, pyrazolate, and azide gave a series of complexes **6**–**11**, respectively. UV–vis, electrochemistry, and EPR data are presented for these dicopper complexes. Variable-temperature magnetic susceptibility data are presented for complexes **5**, **7**, **9**, and **10**. The parent complex, **5**, is weakly ferromagnetic ($2J$ = 4.2 cm^{-1}); complex **7** is paramagnetic ($2J$ = 0.0 cm^{-1}), while **9** and **10** are weak antiferromagnets (**9**, $2J$ = −4.9 cm^{-1}; **10**, $2J$ = −77.8 cm^{-1}). The spectral and magnetic properties are discussed in the context of the known solid-state structure of **5**. The suitability of these complexes as models for the dicopper site of hemocyanin is discussed, and the implications for model design are considered.

Introduction

Inorganic chemists have contributed to the understanding of metalloproteins by the preparation and study of low molecular weight compounds designed to mimic both the structure and chemistry of metal ions in biology.[1] This "bioinorganic" or "biomimetic" approach has recently been applied to a number of copper-containing proteins.[2] One such system is the dicopper protein hemocyanin (Hc).[3-15] The function of this "type 3" copper enzyme is to bind and transport molecular oxygen in the hemolymph of molluscs and arthropods. The nature of the copper site is not entirely clear; however, EXAFS,[16,17] resonance Raman,[18] and other physicochemical studies[19-21] suggest that each copper ion in the oxy form of the protein is pentacoordinate. The coordination sphere is thought to include two or three imidazole (histidine) ligands, an endogenous oxygen atom bridge, and a peroxide moiety as in **1**. The source of the bridging oxygen is

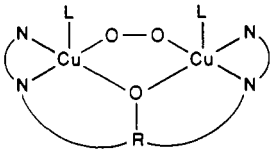

1

the subject of considerable speculation. Initially, it was postulated to be a phenolate oxygen from a tyrosine residue. However, recent crystallographic studies on deoxy-Hc call into question these earlier speculations and suggest that phenolate is not the bridging group.[22] The Cu–Cu separation is 3.67 Å.[16,17] In oxy-Hc, the bridging ligands presumably mediate antiferromagnetic coupling between the copper atoms, resulting in the observed diamagnetism at room temperature. An EPR-detectable met form of Hc (Cu(II)–Cu(II)) is also known.[2] Early approaches to modeling this dicopper center utilized Schiff bases or other unsaturated ligands.[23] Recently, attention has focused on complexes that are designed to better mimic the biological environment of the copper ions in hemocyanin.[3-15] To this end, we have prepared the ligand 2,6-bis-[(bis(benzimidazolylmethyl)amino)methyl]-*p*-cresol (**4**).[14]

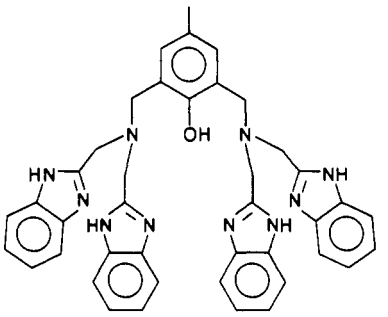

4

In this paper, we describe the synthesis of **4** and a series of derivatives of **4** containing a variety of exogenous ligands. The

* To whom correspondence should be addressed.
† Part 1 to be considered ref 14.

(1) Holm, R. H.; Ibers, J. A. *Science* (*Washington, D.C.* **1980**, *209*, 223.
(2) Spiro, T., Ed. *Copper Proteins, Metal Ions in Biology*; 1981; Vol. 3.
(3) Sorrell, T. N.; O'Connor, C. J.; Anderson, O. P.; Reibenspies, J. H. *J. Am. Chem. Soc.* **1985**, *107*, 4199.
(4) Sorrell, T. N.; Jameson, D. L.; O'Connor, C. J. *Inorg. Chem.* **1984**, *23*, 190.
(5) McKee, V.; Zvagulis, M.; Reed, C. A. *Inorg. Chem.* **1985**, *24*, 2914.
(6) McKee, V.; Zvagulis, M.; Dagdigian, J. V.; Patch, M. G.; Reed, C. A. *J. Am. Chem. Soc.* **1984**, *106*, 4765.
(7) McKee, V.; Dagdigian, J. V.; Bau, R.; Reed, C. A. *J. Am. Chem. Soc.* **1981**, *103*, 7000.
(8) Karlin, K. D.; Cohen, B. I. *Inorg. Chim. Acta* **1985**, *107*, L17.
(9) Karlin, K. D.; Shi, J.; Hayes, J. C.; McKown, J. W.; Hutchinson, J. P.; Zubieta, J. *Inorg. Chim. Acta* **1984**, *91*, L3.
(10) Suzuki, M.; Uehara, A. *Inorg. Chim. Acta* **1984**, *87*, L29.
(11) Suzuki, M.; Kanatomi, H.; Murase, I. *Bull. Chem. Soc. Jpn.* **1984**, *57*, 36.
(12) Karlin, K. D.; Dalstrom, P. L.; Cozzette, S. N.; Scensny, P. M.; Zubieta, J. *J. Chem. Soc., Chem. Commun.* **1981**, 881.
(13) Karlin, K. D.; Haka, M. S.; Cruse, R. W.; Gultneh, Y. *J. Am. Chem. Soc.* **1985**, *107*, 5828.
(14) Berends, H. P.; Stephan, D. W. *Inorg. Chim. Acta* **1985**, *99*, L53.
(15) Nishida, Y.; Shimo, H.; Machara, H.; Kida, S. *J. Chem. Soc., Dalton Trans.* **1985**, 1945.
(16) Brown, J. M.; Powers, L.; Kincaid, B.; Larrabee, J. A.; Spiro, T. G. *J. Am. Chem. Soc.* **1980**, *102*, 4210.
(17) Woolerty, G. L.; Powers, L.; Winkler, M.; Solomon, E. I.; Spiro, T. G. *J. Am. Chem. Soc.* **1984**, *106*, 86.
(18) Larrabee, J. A.; Spiro, T. G. *J. Am. Chem. Soc.* **1980**, *102*, 4217.

0020-1669/87/1326-0749$01.50/0

spectral, electrochemical, and magnetic properties of these dicopper complexes are presented. The relevance of these compounds to the Hc active site and the implications for model design are discussed.

Experimental Section

All solvents used in the preparations were freshly distilled. Melting points were recorded on a Fisher stage melting point apparatus and are not corrected. ^{1}H NMR spectra were recorded on a Varian EM-360 spectrometer operating at 60 MHz. Chemical shifts are reported in ppm relative to the internal reference $Si(CH_3)_4$. UV–vis absorption spectra were recorded on a Hewlett-Packard 8451A diode array spectrophotometer. X-band EPR spectra were recorded on a Varian E-12 spectrometer. Additional EPR spectra were recorded on a Varian E-3 spectrometer connected to a Digital PDP 11 computer located at the University of California (Santa Cruz). EPR spectra were recorded on solid samples at 298 K or on frozen solutions at 77 K. Electrochemical experiments were performed on a BAS CV-27 cyclic voltammeter using a glassy carbon or Pt working electrode and acetonitrile or DMF as the solvent. $[NEt_4][ClO_4]$ was used as the supporting electrolyte. All potentials were recorded at 298 K vs. a saturated calomel electrode. Electrochemical data are deposited in Table S1 (supplementary material). IR spectra were recorded on a Nicolet FTIR 5DX spectrometer. Elemental analyses were performed by the Guelph Chemical Laboratories, Guelph, Ontario, Canada. Compound **2**, bis(benzimidazolylmethyl)amine, was prepared by the published method.[24]

Magnetic Susceptibility Measurements. Magnetic susceptibility measurements were made with an SHE Corp. VTS susceptometer (900 series) located at the Francis Bitter National Magnet Laboratory, Cambridge, MA. These measurements were made in the 6–300 K range. The magnetic susceptibility of the sample bucket was measured over the full temperature range. The magnetic data for the samples were then corrected for the diamagnetic contribution from the bucket. Magnetic susceptibility measurements were made on polycrystalline samples weighing 20–30 mg. The magnetic susceptibility was corrected for ligand diamagnetism, which was calculated by using Pascal's constants.[25,26] A temperature-independent paramagnetism (TIP) term of $+30 \times 10^{-6}$ cgsu/Cu atom was included.[6] Exchange interactions between the Cu ions are given in terms of the isotropic spin Hamiltonian, $\mathcal{H} = -2J\mathbf{S}_1\cdot\mathbf{S}_2$. $2J$ and the theoretical molar susceptibilities χ_m were calculated from a nonlinear least-squares fit of the Bleaney–Bowers equation (1)[26] to the

$$\chi = \left[\frac{2Ng^2\mu_B{}^2}{3kT}\right]\left[\frac{1}{1 + [\exp(-2J/kT)]/3}\right] \quad (1)$$

data. The symbols have their usual meaning.[25,26] In the case of the antiferromagnet **10**, the χ_m values were corrected for the presence of 2.28% of paramagnetic impurity with $S = {}^1/_2$. The diamagnetic corrections, observed χ, $1/\chi$, and calculated values of χ and $1/\chi$ are reported in supplementary tables (Tables S2–S5) for compounds **5**, **7**, **9**, and **10**. Data obtained for **11** were qualitatively consistent with a weak antiferromagnet; however, the presence of paramagnetic impurities made a quantitative treatment unreliable.

Preparation of 2,6-Bis(chloromethyl)-*p*-cresol (3). This compound was prepared by a modification of the method of Sorrell et al.[4] Dry HCl gas was passed through a suspension of 2,6-bis(hydroxymethyl)-*p*-cresol (10.0 g, 60 mmol) in 250 mL of dry diethyl ether for 40 min. The clear yellow solution was allowed to stir for 1 h. The solvent was removed in vacuo, and the crude product was recrystallized from hexane, yielding beige needles (11.1 g, 91%). Mp 84 °C (lit. 87 °C).[4]

Preparation of 2,6-Bis[(bis(benzimidazolylmethyl)amino)methyl]-*p*-cresol (4). A solution of **3** (2.28 g, 11 mmol) in 10 mL of methanol was added dropwise to a cold solution of **2** (6.1 g, 22 mmol) and triethylamine (2.2 g, 22 mmol) in methanol (60 mL). The solution was heated to reflux for 15 min. After dissolution of the suspended material, a fine white precipitate appeared. The heat was removed and the reaction mixture stirred for 24 h at 25 °C. The white precipitate was filtered off, washed with cold ether (10 mL), and air-dried: yield 4.0 g (49%); mp 178 °C. ^{1}H NMR ($(CD_3)_2SO$) δ: 7.3 (m, 18 H), 5.7 (s, 1 H), 3.9 (s, 4 H), 4.1 (s, 8 H), 3.4 (s, 4 H), 2.3 (s, 3 H). Anal. Calcd for $C_{41}H_{41}N_{10}O_2Cl$: C, 66.43; H, 5.57; N, 18.89. Found: C, 67.30; H, 5.79; N, 18.79.

Preparation of $[Cu_2L(H_2O)_2][ClO_4]_3\cdot 3H_2O$ (5). A suspension of **4** (100 mg, 0.135 mmol) in methanol (10 mL) was mixed with 10 mL of a methanolic solution containing $[Cu(H_2O)_4][ClO_4]_2$ (100 mg, 0.27 mmol). After the mixture was allowed to stand at 25 °C, 93 mg (57%) of green-brown crystals of **5** were deposited. UV–vis (CH_3OH; λ, nm (ϵ, M^{-1} cm^{-1})): 212 (17 100), 244 (23 200), 274 (26 300), 280 (24 800), 300 (5050), 466 (466), 714 (137). Anal. Calcd for $C_{41}H_{47}N_{10}O_{18}Cu_2Cl_3$: C, 40.99; H, 3.94; N, 11.66. Found: C, 40.48; H, 3.95; N, 11.34.

Preparation of $[Cu_2L(MeIm)(H_2O)][ClO_4]_3\cdot 3H_2O$ (6). To a solution of **5**, prepared as above, was added *N*-methylimidazole (MeIm) (11 mg, 0.135 mmol). Deep blue crystals were isolated by filtration after cooling to 4 °C: yield 80 mg (45%). UV–vis (CH_3OH; λ, nm (ϵ, M^{-1} cm^{-1})): 212 (83 000), 245 (28 400), 274 (29 000), 280 (27 500), 302 (5540), 676 (172). Anal. Calcd for $C_{45}H_{51}N_{12}O_{17}Cu_2Cl_3$: C, 42.71; H, 4.06; N, 13.28. Found: C, 42.73; H, 3.88; N, 13.78.

Preparation of $[Cu_2L(py)_2][ClO_4]_3\cdot 4H_2O$ (7). A solution of **5** was prepared as described above, and pyridine (py) (21 mg, 0.27 mmol) was added. Dark brown-blue crystals deposited on standing at 4 °C: yield 127 mg (71%). UV–vis (CH_3OH; λ, nm (ϵ, M^{-1} cm^{-1})): 210 (83 300), 246 (28 500), 274 (29 200), 280 (27 500), 300 (5200), 445 (489), 672 (181). Anal. Calcd for $C_{51}H_{55}N_{12}O_{17}Cu_2Cl_3$: C, 45.66; H, 4.13; N, 12.53. Found: C, 45.72; H, 4.01; N, 12.17.

Preparation of $[Cu_2L(X)][ClO_4]_2\cdot 3H_2O$ (X = HCO_2^- (8), $CH_3CO_2^-$ (9), $C_3H_3N_2^-$ (10), N_3^- (11)). These compounds were prepared by following the procedure described for **6** with sodium formate (92 mg, 0.135 mmol), sodium acetate (11 mg, 0.135 mmol), sodium pyrazolate (12 mg, 0.135 mmol), or sodium azide (8.8 mg, 0.135 mmol) replacing the MeIm. After the mixtures were allowed to stand at room temperature, each of these compounds crystallized from solution. **8**: brown microcrystalline solid; yield 80 mg (53%). UV–vis (CH_3OH; λ, nm (ϵ, M^{-1})): 210 (80 400), 244 (24 500), 274 (27 300), 280 (26 100), 302 (4170), 440 (753) sh, 706 (153). Anal. Calcd for $C_{42}H_{44}N_{10}O_{14}Cu_2Cl_2$: C, 45.41; H, 3.99; N, 12.61. Found: C, 45.65; H, 3.89; N, 12.88. **9**: green-brown microcrystalline solid; yield 74 mg (49%). UV–vis (CH_3OH; λ, nm (ϵ, M^{-1} cm^{-1})): 210 (84 500), 242 (30 000), 274 (31 700), 280 (30 200), 300 (10 600), 454 (842), 692 (208). Anal. Calcd for $C_{43}H_{46}N_{10}O_{14}Cu_2Cl_2$: C, 45.91; H, 4.12; N, 12.45. Found: C, 46.07; H, 3.92; N, 11.88. **10**: dark green blocks; yield 135 mg (88%). UV–vis (CH_3OH; λ, nm (ϵ, M^{-1} cm^{-1})): 212 (86 200), 242 (28 800), 274 (28 800), 280 (27 500), 308 (3610), 452 (644), 634 (235), 730 (199). Anal. Calcd for $C_{44}H_{46}N_{12}O_{12}Cu_2Cl_2$: C, 46.65; H, 4.09; N, 14.84. Found: C, 46.93; H, 3.78; N, 14.85. **11**: brown microcrystalline solid; yield 70 mg (52%). UV–vis (CH_3OH; λ, nm (ϵ, M^{-1} cm^{-1})): 212 (91 100), 244 (28 900), 274 (32 300), 280 (30 700), 302 (5540), 430 (806), 684 (215). Anal. Calcd for $C_{41}H_{43}Cl_2Cu_2N_{13}O_{12}$: C, 44.45; H, 3.91; N, 16.44. Found: C, 45.06; H, 3.88; N, 15.91.

Results and Discussion

Compound **4** is prepared by reaction of the dichloro species **3** with the secondary amine **2**. This heptadentate ligand was designed to mimic some of the features of the copper binding site in Hc. The cresol moiety provides a phenoxide group to mimic the endogenous oxy bridge. Benzimidazole groups act as analogues of the histidine residues that bind Cu in the native protein. In addition, the ligand was contrived to add steric bulk about the dicopper site. By creating this protective envelope, it may be possible to stabilize species containing small molecules as bridging substrates.

Reaction of **4** with $[Cu(H_2O)_6][ClO_4]_2$ produced the green-brown dicopper complex **5** in reasonable yields. The formulation of **5** has been previously confirmed by X-ray crystallography.[14] The results of the structural study of **5** show that within the trication each copper atom is coordinated to an amine, two benzimidazole nitrogen atoms, a bridging phenoxide oxygen, and an oxygen atom of a water molecule. The two pseudo-square-pyramidal copper atoms are not in equivalent environments, despite the fact that the atoms comprising the coordination spheres of

(19) (a) Himmelwright, R. S.; Eickman, N. C.; LuBien, C. D.; Solomon, E. I. *J. Am. Chem. Soc.* **1980**, *102*, 5278. (b) Himmelwright, R. S.; Eickman, N. C.; Solomon, E. I. *Ibid.* **1979**, *101*, 1576.
(20) Wilcox, D. E.; Long, J. R.; Solomon, E. I. *J. Am. Chem. Soc.* **1984**, *106*, 2186.
(21) Solomon, E. I.; Penfield, K. W.; Wilcox, D. E. *Struct. Bonding (Berlin)* **1983**, *53*, 1.
(22) (a) Linzen, B.; Soeter, N. M.; Riggs, A. F.; Schneider, H. J.; Schartau, W.; Moore, M. D.; Yokota, E.; Behrens, P. Q.; Nakashima, H.; Takagi, T.; Neomoto, T.; Vereijken, J. M.; Bak, H. J.; Beintema, J. J.; Volbeda, A.; Gaykema, W. P. J.; Hol, W. G. J. *Science (Washington, D.C.)* **1985**, *209*, 519. (b) Gaykema, W. P. J.; Volbeda, A.; Hol, W. G. J. *J. Mol. Biol.* **1985**, *187*, 255. (c) Gaykema, W. P. J.; Hol, M. G. J.; Vereijken, J. M.; Soeter, N. M.; Bak, H. J.; Beintema, J. J. *Nature (London)* **1984**, *309*, 23.
(23) Casellato, U.; Vigato, P. A. *Coord. Chem. Rev.* **1971**, *23*, 31.
(24) Berends, H. P.; Stephan, D. W. *Inorg. Chim. Acta* **1984**, *93*, 173.
(25) Drago, R. S. *Physical Methods on Chemistry*; Saunders: Philadelphia, PA, 1977.
(26) Carlin, R. L. *Magnetochemistry*; Springer-Verlag: New York, 1986.

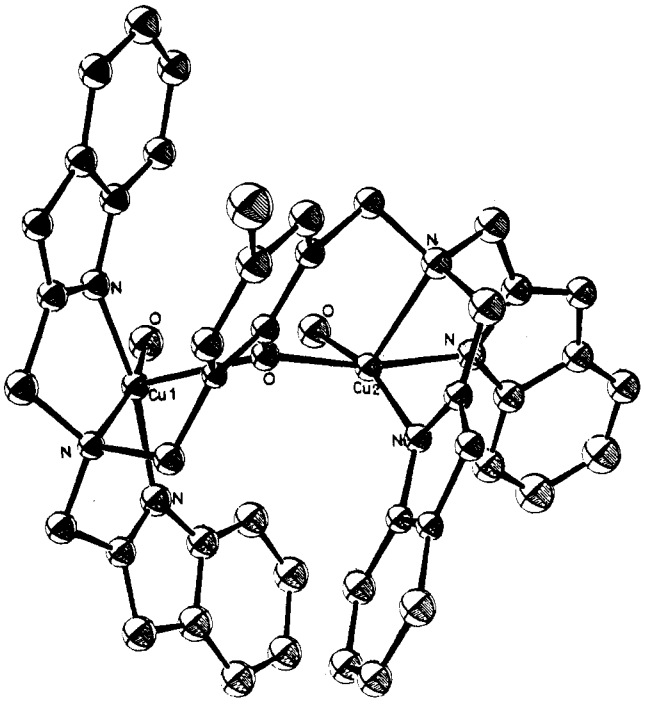

Figure 1. ORTEP drawing of the trication of **5**. 50% thermal ellipsoids are shown, and hydrogen atoms are omitted for clarity.

the two copper atoms are identical. One N_3 portion of the ligand **4** adopts a meridial geometry about Cu1, while the other N_3 fragment is facial about Cu2. The bridging phenoxide oxygen atom is in the equatorial plane of the coordination sphere of Cu2 while in the axial position for Cu1. The square planes of the copper coordination spheres are not coplanar. The dihedral angle between these planes is 64.7°. The Cu–Cu separation is 3.785 Å. Sorrell et al.[3] have recently noted that Cu–Cu separations of ca. 3.1 Å are seen in other ligand systems based on the 2,6-bis(methylamino)cresol moiety. The substantial increase in the metal–metal distance observed in the present system is caused by the inclusion of two features in **4**. First, the short distances between the amine N atom and the benzimidazole N atoms require the formation of two adjacent five-membered rings for binding of each Cu ion. This results in a strained geometry about the Cu ions, which is accommodated by opening of the Cu–O–Cu angle and thus a larger Cu–Cu separation. Also important in increasing the metal–metal distance are the steric interactions among benzimidazole groups. Such interactions are presumably minimized by the increased Cu–Cu distance. Thus, some of the features of **4** present alternative strategies to those offered by Sorrell et al.[3] in efforts to achieve Cu–Cu separations of greater than 3.5 Å. An ORTEP drawing of the trication of **5** is shown in Figure 1.

Preliminary results from a single-crystal EPR study[27] of **5** provide insight into the mechanism of complex formation. In addition to the EPR signal of the dimer **5**, a weak but discernible signal arising from a monomeric Cu species is observed. This signal arises from binding of Cu in the Cu1 site exclusively (Figure 1). The trans geometry of the benzimidazole groups presumably minimizes steric interactions upon initial binding of Cu. On binding of the second Cu atom, a cis arrangement of the benzimidazole groups about Cu2 minimizes steric interactions of the ligand fragments with the remainder of the complex. Thus, it seems that complexation of Cu by **4** occurs in a specific, stepwise manner.

Solutions of **5**, generated in situ, react with a variety of exogenous ligands. One or both of the coordinated water molecules of **5** can be replaced by reaction with *N*-methylimidazole or pyridine, thus yielding complexes **6** and **7**, respectively. Alternatively, the water molecules of **5** can be replaced with bridging anionic ligands. Reactions with formate, acetate, pyrazolate, and azide afford complexes **8**–**11**, respectively. These complexes were characterized by UV–vis, EPR, magnetic susceptibility, electrochemistry, and combustion analyses. Data for each species, **5**–**11**, are consistent with the formulations given.

Absorption Spectra. The major features observed in the UV–vis spectra are shown in Figure 2. All the complexes showed absorptions in the region 200–300 nm. These bands are attributable to ligand absorptions. In the visible region, a band in the range 430–470 nm was observed for complexes **5**–**11**. This band is assigned to phenoxide-to-metal charge transfer (CT). Previously, bands at 425 and 440–450 nm have been attributed to the presence of bridging phenoxide in hemocyanin[2] and related model compounds,[3,4,8,10,12] respectively. Bands at ca. 410–545 nm have been assigned to phenoxide-to-Cu CT in mononuclear Cu complexes.[8,28] In the case of **11**, the increased ϵ value for this band may arise from overlap with $N_3^- \rightarrow$ Cu CT.

The azide derivative of met-Hc exhibits absorption maxima at 350 ($\epsilon \simeq 1500$ M^{-1} cm^{-1}) and 710 nm ($\epsilon \simeq 200$ M^{-1} cm^{-1}).[2] In comparison, the model compound **11** shows no distinct maximum at 350 nm, yet the ϵ at 350 nm is ca. 1700 M^{-1} cm^{-1}. An absorption at 684 nm ($\epsilon = 215$ M^{-1} cm^{-1}) is also seen. By analogy, these absorptions are assigned to LMCT and d–d transitions, respectively. The infrared spectrum of **11** shows asymmetric stretches of azide at 2084 and 2042 cm^{-1}. This observation suggests the presence of two types of bound azides. Repeated recrystallizations did not effect a separation of the two types of complexes. The azide stretch for azido-met-Hc occurs at 2042 cm^{-1} and is thought to arise from the presence of a μ-1,3-azido bridge between the Cu ions.[2] For model complexes, the azide stretching frequency is reported not to be diagnostic of the binding mode.[29] Comparison of the IR data for **11** with those of other models[3,6,7,30–32] suggests **11** is a mixture containing a μ-1,3-azido-bridged complex as well as a second compound containing perhaps an end-on-bound azide. The Cu–Cu separation in **5** suggests that a μ-1,3-bridging mode could be adopted with minimal alteration of the geometry. While a μ-1,1-azido bridge is another possibility, the substantial change in geometry that would be required makes this seem unlikely. Magnetic susceptibility data indicate qualitatively the presence of both antiferromagnetic and paramagnetic material. Charlot et al. have recently shown that antiferromagnetic behavior is expected from dimeric copper complexes containing μ-1,3-azido bridges.[33] End-on azide binding would lead to two distinct Cu environments and thus give rise to weak ferromagnetism or paramagnetism. The notion of a mixture of azide-binding modes is further supported by the EPR data in which the superposition of signals arising from monomeric and dimeric copper complexes is observed.

Electrochemistry. Compounds **5**–**11** have been studied by cyclic voltammetry. The data are deposited in Table S1. All of the compounds show similar features. Each compound undergoes nonreversible reductions in the range 0.0 to −0.50 V vs. SCE. Studies done in acetonitrile using a Pt electrode gave the best definition of the electrochemical features. For **5**, **8**, **9**, **10**, and **11** two distinct yet broad reduction peaks were observed. In the case of **6** and **7** a single broad wave was seen. The range of potentials seen is typical of reduction of Cu(II) to Cu(I).[34–37] The

(27) Ozarowski, A.; McGarvey, B. R., unpublished results.

(28) Ainscough, E. W.; Bingham, A. G.; Brodie, A. M.; Husbands, J. M.; Plowman, J. E. *J. Chem. Soc., Dalton Trans.* **1981**, 1701.
(29) Karlin, K. D.; Hayes, J. C.; Hutchinson, J. P.; Zubieta, J. *J. Chem. Soc., Chem. Commun.* **1983**, 376.
(30) Lorsch, J.; Paulus, H.; Haase, W. *Inorg. Chim. Acta* **1985**, *106*, 101.
(31) Agnus, Y.; Louis, R.; Weiss, R. *J. Am. Chem. Soc.* **1979**, *101*, 3381.
(32) Drew, M. G. B.; Nelson, J.; Esho, F.; McKee, V.; Nelson, S. M. *J. Chem. Soc., Dalton Trans.* **1982**, 1837.
(33) Charlot, M. F.; Kahn, O.; Chaillet, M.; Larrieu, C. *J. Am. Chem. Soc.* **1986**, *108*, 2574.
(34) Gagne, R. R.; Koval, C. A.; Smith, T. J.; Cinolino, M. C. *J. Am. Chem. Soc.* **1979**, *101*, 4571.
(35) Fenton, D. E.; Schroeder, R. R.; Linvedt, R. L. *J. Am. Chem. Soc.* **1978**, *100*, 1931.
(36) Latour, J. M.; Limosin, D.; Tandon, S. S. *Inorg. Chim. Acta* **1985**, *107*, L1.
(37) Addison, A. W. *Inorg. Nucl. Chem. Lett.* **1976**, *12*, 899.

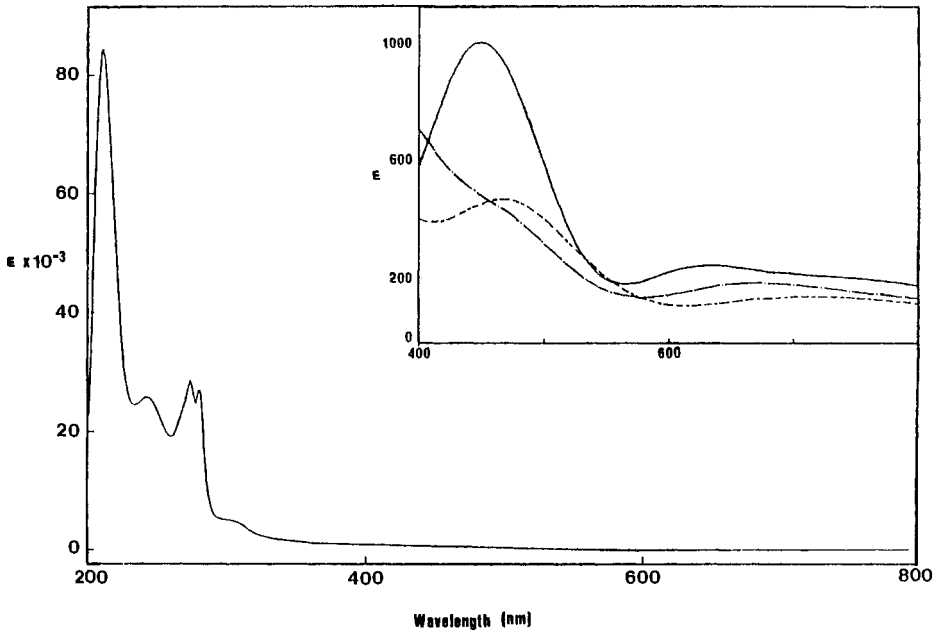

Figure 2. UV–vis spectrum of **5**. Insert: **5** (---); **7** (– – –); **10** (—).

Table I. EPR and Magnetic Susceptibility Parameters

cmpd	T, K[a]	g	$2J$, cm^{-1}
5	298	2.14, 4.55	+4.2
	77	2.09	
6	298	2.14, 4.5	
	77	2.15	
7	298	2.11, 4.48	0.0
	77	2.12	
8	298	2.06, 7.2	
	77	2.2, 4.8	
9	298	2.09, 6.86	−4.9
	77	2.23, 4.76	
10	298	2.13, 4.5–5.0	−77.8
11	298	2.06	

[a] Spectral data given for T = 298 K were recorded on polycrystalline samples; data given for T = 77 K were recorded on frozen methanolic solutions.

presence of two reduction potentials is expected for two consecutive one-electron processes. Oxidation of the compounds occurs in a quasi-reversible manner at potentials of ca. 0.80–1.10 V vs. SCE. The exact nature of the oxidation product is not clear. Cu(II-I)–Cu(II) couples are known to occur in this potential range.[38] Alternatively, this feature could arise from ligand oxidation. The ligand **4** alone shows no reversible oxidation, but the possibility of metal-mediated ligand oxidation cannot be ruled out. The nature of this oxidation is the subject of ongoing work.

EPR Spectra. Representative EPR spectra are shown in Figure 3. Spectral parameters are given in Table I. The EPR spectrum of polycrystalline **5** (Figure 3a) shows a broad signal with g_{av} = 2.11. A half-field transition is observed at g = 4.5. Zero-field-splitting effects are evident. The magnitudes of D and E that contribute to the zero-field splitting are approximately 0.00 and 0.0542 cm^{-1}, respectively. The values of these parameters will be more accurately determined in the course of a single-crystal EPR study.[27]

The EPR spectrum of a frozen methanolic solution of **5** (Figure 3b) shows a broad axial-Cu signal. Although the hyperfine structure is weakly resolved, there appears to be two sets of peaks. These are consistent with the presence of two different, but similar, Cu environments. This spectrum of **5** is similar to that seen for the EPR-detectable form of met-Hc.[2] Other data suggest that no endogenous bridge exists between the copper ions in met-Hc.

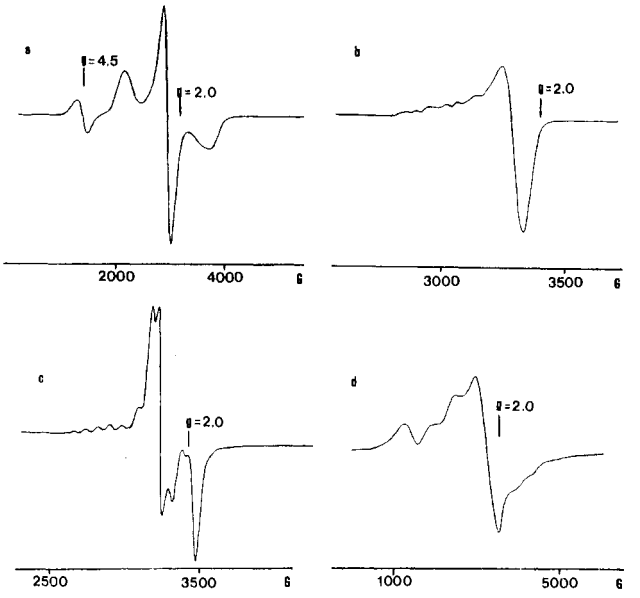

Figure 3. Selected EPR Spectra: (a) polycrystalline **5** (298 K); (b) methanol solution of **5** (77 K); (c) methanol solution of **7** (77 K); (d) polycrystalline **10** (298 K).

Nonetheless, the present result suggests that the model compound produces Cu coordination spheres similar to those in the protein, even though the proximity of the metal centers in the model may be inappropriate.

The EPR data for both solid and frozen solutions of **6** and **7** show triplet spectra with g_{av} = 2.12 (Figure 3c). The average hyperfine splitting parameter ($A_{\parallel}$) is approximately 80 G (0.007 48 cm^{-1}). In contrast to that observed for **5**, it is apparent that zero-field-splitting parameters are small compared to the anisotropy of the **g** tensor. Zero-field-splitting parameters have been related to interactions between ground and excited states of the adjacent Cu atoms in other dimeric Cu systems.[39] However, in the present system it is not clear how ligand substitution affects such interactions.

EPR spectra of **8** and **9** are similar to those seen for **5**. Broad signals with g_{av} = 2.08 and $g \simeq 7$ are observed in both cases. The EPR spectra of frozen solutions of **8** and **9** show broad axial-Cu

(38) Bossu, F. P.; Chellappa, K. L.; Margerum, D. W. *J. Am. Chem. Soc.* **1977**, *99*, 2195.

(39) Ozarowski, A.; Reinen, D. *Inorg. Chem.* **1986**, *25*, 1704.

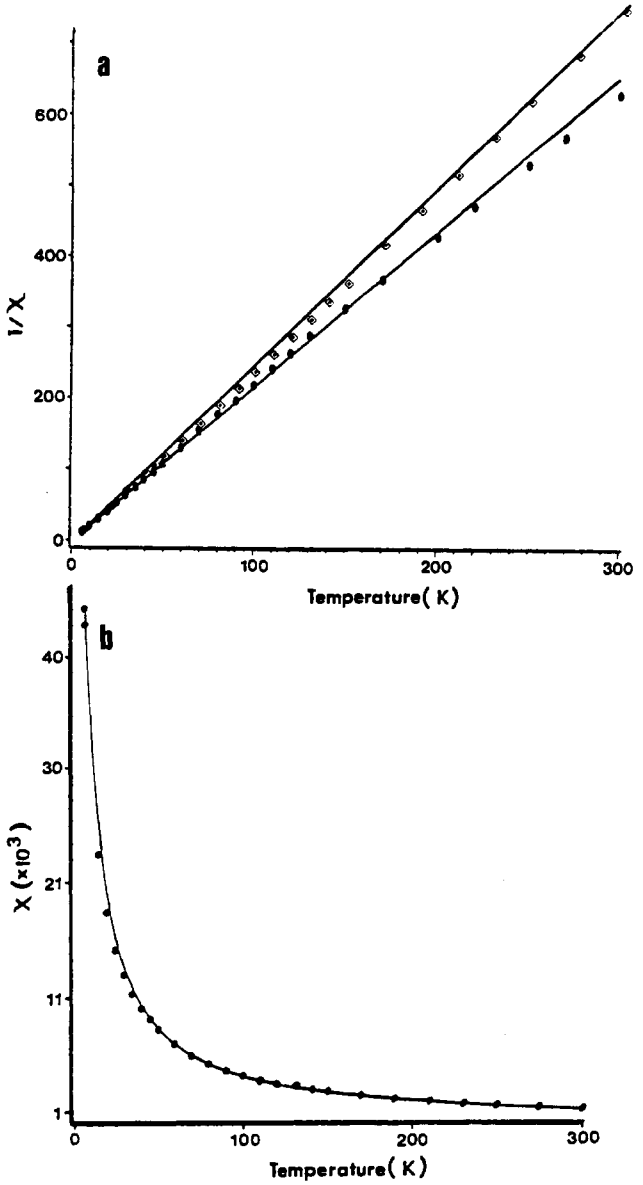

Figure 4. (a) $1/\chi$ vs. T for **5** (dots) and **7** (squares). (b) χ vs. T for **9**. In each plot the individual points are experimentally measured data while the solid lines are the least-squares fit of the data to the Bleaney–Bowers equation.

signals. The similarity of the spectra of **5**, **8**, and **9** may result from the similarity of the Cu coordination spheres. The increase in zero-field splitting for **8** and **9** may arise from a change in the Cu–Cu distance. This is expected, as the oxygen–oxygen distance (i.e., between coordinated H_2O molecules) in **5** is 2.8 Å while in a carboxylate group the O–O distance is 2.2 Å.

The EPR spectrum of solid **10** also shows features similar to the triplet spectrum of **5**. A broad signal with $g_{av} = 2.13$ and a half-field transition at $g \simeq 4.5$ are seen. This similarity is interesting since **5** and **10** are ferromagnetic and antiferromagnetic, respectively (vide infra). These observations suggest that, for the present compounds, the metal–metal interactions responsible for superexchange have little effect on the zero-field splitting. A similar observation has been made for other dimeric Cu systems.[39]

Magnetic Susceptibility. Complex **5** obeys the Curie law. A plot of $1/\chi$ vs. T for **5** is shown in Figure 4a. The regression analysis of χ using the Bleaney–Bowers equation gives $2J = 4.2$ cm^{-1}, which is indicative of a weak ferromagnet. The g value used in the fit was 2.20. This compares to 2.11 derived from the EPR data. This discrepancy may arise from small inaccuracies in the molecular weight due to loss of H_2O of crystallization.

The pyridine complex **7** obeys the Curie–Weiss law and is paramagnetic. A graph of $1/\chi$ vs. T for **7** is included in Figure 4a. Analysis of the magnetic susceptibility data yields $2J = 0$ cm^{-1}, $g = 2.11$, and $\theta = -2.34$ K. Complex **9** is very weakly antiferromagnetic with $2J = -4.9$ cm^{-1} and $g = 2.12$ χ vs. T data for **9** are shown in Figure 4b. Complex **10** exhibits typical antiferromagnetism (Figure 5) with $2J = -77.8$ cm^{-1}, $g = 2.10$, and $\theta = -5.0$ K.

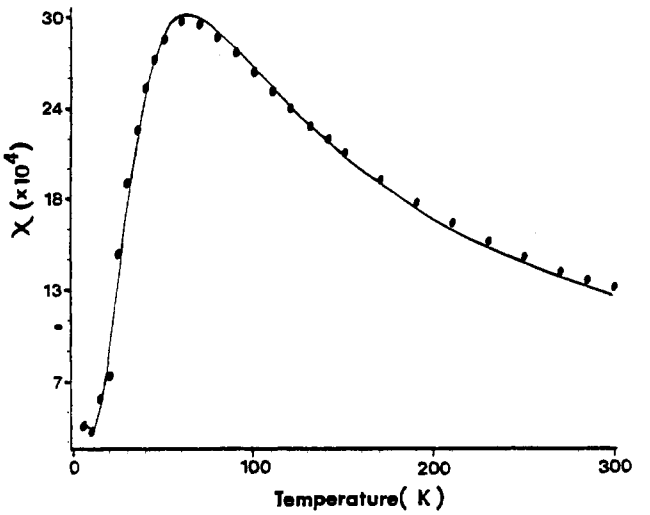

Figure 5. χ vs. T for **10**. The individual points are experimentally measured data while the solid line is the least-squares fit of the data to the Bleaney–Bowers equation.

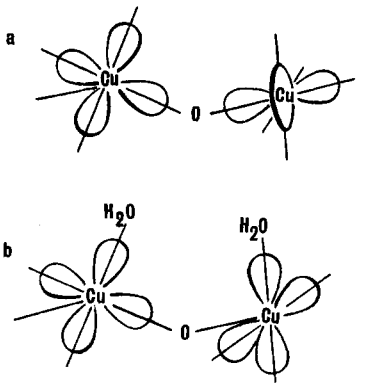

Figure 6. Orientation of the atomic orbitals in compound **5** involved in (a) bonding to the bridging phenoxide oxygen atom (d_{z^2} and $d_{x^2-y^2}$ orbitals on Cu1 and Cu2) and (b) bonding to the exogenous water molecules ($d_{x^2-y^2}$ orbitals of the Cu atoms).

Magnetic interactions between Cu ions in binuclear complexes are strongly structure dependent. In the present complexes, some understanding of the magnetostructural relationship can be obtained. For complex **5**, precise structural and magnetic data are available. Both Cu ions are in a pseudo-square-pyramidal geometry and thus will have $d_{x^2-y^2}$ ground states. Direct electronic communication is necessary for an antiferromagnetic interaction. The bridging phenoxide oxygen, being in the axial position relative to Cu1 and equatorial to Cu2, has bonding interactions with the d_{z^2} and $d_{x^2-y^2}$ orbitals of Cu1 and Cu2, respectively (Figure 6). Thus the oxygen atom does not mediate an interaction between the ground states and weak ferromagnetism results.

No precise structural data are available for complexes **6–11**; however, inferences regarding the magnetostructural relationship can be made on the basis of the structure of the parent compound **5**. If it is assumed that no major structural changes occur on binding of an exogenous ligand to **5**, then the magnetic interactions between ground-state $d_{x^2-y^2}$ orbitals of the Cu atoms will be mediated primarily through the exogenous ligand. The principle of "orbital complementarity" has been used by Reed et al.[5] to illuminate the magnetostructural correlations in other Hc model systems. In the present complexes, orbital complementarity can be attained for both the acetate- and pyrazolate-bridged complexes (Figure 7). This is true because, unlike those of the system

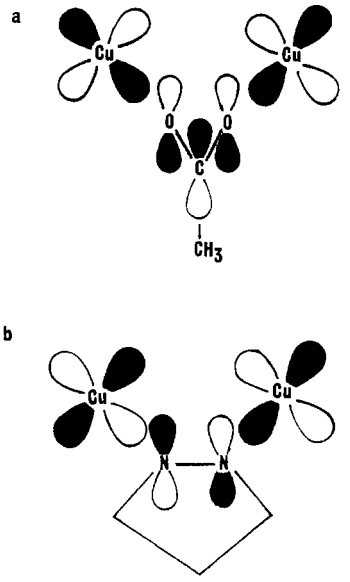

Figure 7. Orbital complementarity for binding of bridging (a) acetate and (b) pyrazolate between the Cu atoms.

described by Reed, the polarities of the $d_{x^2-y^2}$ orbitals in the present compounds are not restricted by the bridging phenoxide oxygen atom. The presence of only a single ligand mediating the magnetic interaction between the Cu atoms results in the relatively weak antiferromagnetism of complexes **9** and **10**. It appears that a bridging pyrazolate group is capable of effecting a stronger antiferromagnetic interaction between the participant metals than a bridging acetate group.

Summary. The system described and characterized herein provides some important features for an effective Hc model. The metal coordination spheres, Cu-Cu separations, spectroscopic properties, and reactivity with small-molecule substrates indicate that **5** is a reasonable model for the binuclear Cu site of EPR-detectable forms of met-Hc. Magnetic properties of the derivatives of **5**, in which exogenous ligands have been incorporated, do not mimic the protein derivatives. It is apparent that these complexes do not adopt an orientation in which a strong superexchange interaction between the Cu atoms occurs. Modifications of this system designed to encourage such interactions are the subject of current interest.

Acknowledgment. The NSERC of Canada is thanked for financial support of this research. Dr. P. E. Doan, Dr. A. Ozarowski (University of Windsor), and Dr. P. K. Mascharak (University of California, Santa Cruz) are thanked for assistance in recording EPR spectra. Dr. A. Ozarowski and Dr. P. E. Doan are also thanked for programming assistance. Dr. R. Frankel is thanked for assistance in the operation of the susceptometer at the National Magnet Laboratory. H.P.B. is grateful for the awards of Ontario Graduate and NSERC postgraduate scholarships.

Supplementary Material Available: Electrochemical data (Table S1) and magnetic susceptibility data (Tables S2-S5) (9 pages). Ordering information is given on any current masthead page.

Contribution from the Department of Chemistry, Thimann Laboratories, University of California, Santa Cruz, California 95064, and Department of Chemistry and Biochemistry, University of Windsor, Windsor, Ontario, Canada N9B 3P4

Synthetic Analogue Approach to Metallobleomycins. 2. Synthesis, Structure, and Properties of the Low-Spin Iron(III) Complex of *N*-(2-(4-Imidazolyl)ethyl)pyridine-2-carboxamide

Xiaolin Tao,[†] Douglas W. Stephan,[‡] and Pradip K. Mascharak*[†]

Received October 2, 1986

Reaction of the peptide ligand PypepH (**1**), which resembles part of the metal-chelating section of bleomycins (BLM), with $(Et_4N)[FeCl_4]$ in ethanol affords the iron(III) complex $[Fe(Pypep)_2]Cl\cdot 2H_2O$ (**2**). The structure of this synthetic analogue of Fe(III)-BLM is reported. The complex crystallizes in the triclinic space group $P\bar{1}$ with a = 11.080 (5) Å, b = 9.319 (4) Å, c = 13.665 (5) Å, α = 112.75 (3)°, β = 103.92 (3)°, γ = 73.53 (3)°, and Z = 2. The structure was refined to R = 4.46% by using 1938 unique data ($F_o^2 > 3\sigma(F_o^2)$). The coordination geometry around iron(III) is octahedral with average Fe-N(imidazole) = 1.952 (4) Å and Fe-N(pyridine) = 1.982 (4) Å, respectively. The Fe(III)-N(peptide) bond is 1.957 (4) Å long. The complex is isolated as the *mer* isomer. Variable-temperature Mössbauer spectra and magnetic susceptibility measurement at ambient temperature reveal that the iron is in the +3 oxidation state with a low-spin electronic configuration. The dark red ferric complex (**2**) can be electrochemically and chemically reduced to purple ferrous species. The electronic absorption spectrum of the reduced species is reported.

Introduction

Recently, we have initiated a "synthetic analogue approach"[1] to metallobleomycins (M-BLM) and reported the structures and spectral properties of Cu(II) complexes of two peptides resembling portions of the metal-chelating region of the glycopeptide antibiotics, bleomycins (BLM).[2] Design of suitable yet simple organic frameworks as ligands in these complexes reduced the structural complexities encountered with BLM but retained most of the proposed donor centers around copper in Cu(II)-BLM. Such attempts allowed precise structure determination and correlation between the structure and various spectroscopic properties. Since in vivo DNA damage by BLM is attributed to an iron complex,[3] structural and spectroscopic information on the iron complexes of the synthetic organic fragments is of considerable importance. We report in this paper the synthesis, molecular structure, and spectral properties of the Fe(III) complex of one of the peptides namely, *N*-(2-(4-imidazolyl)ethyl)pyridine-2-carboxamide (**1**). Hereafter, the peptide is abbreviated at PypepH, the dissociable H being the amide H. This tailored ligand mimics three of the six proposed donor centers in Fe(III)-BLM.[3] Though Fe(III)-BLM is incapable of causing DNA strand scission, "activated

[†] University of California.
[‡] University of Windsor.

(1) Ibers, J. A.; Holm, R. H. *Science (Washington, D.C.)* **1980**, *209*, 223.
(2) Brown, S. J.; Tao, X.; Stephan, D. W.; Mascharak, P. K. *Inorg. Chem.* **1986**, *25*, 3377.
(3) Dabrowiak, J. C. *Adv. Inorg. Biochem.* **1983**, *4* and references therein.

0020-1669/87/1326-0754$01.50/0